

Simulation of Melting Ice-Phase Precipitation Hydrometeors for Use in Passive and Active Microwave Remote Sensing Algorithms

Benjamin T. Johnson^{1,2}, William Olson^{1,2}, Gail Skofronick-Jackson²
¹UMBC/JCET, ²NASA/GSFC (Code 612) Contact: jbenjam@umbc.edu

1 Melting Realistically Shaped Particles

Goal: Improved physical realism and similarity to observations

Melting Simulation approach:

- (1) Ice points (blue) with fewest nearest neighbors (NN) melts first.
- (2) If liquid points still have any ice as a NN, it cannot move. This simulates a melt-water coating.
- (3) If liquid points are surrounded by liquid, it can move toward the center of mass.

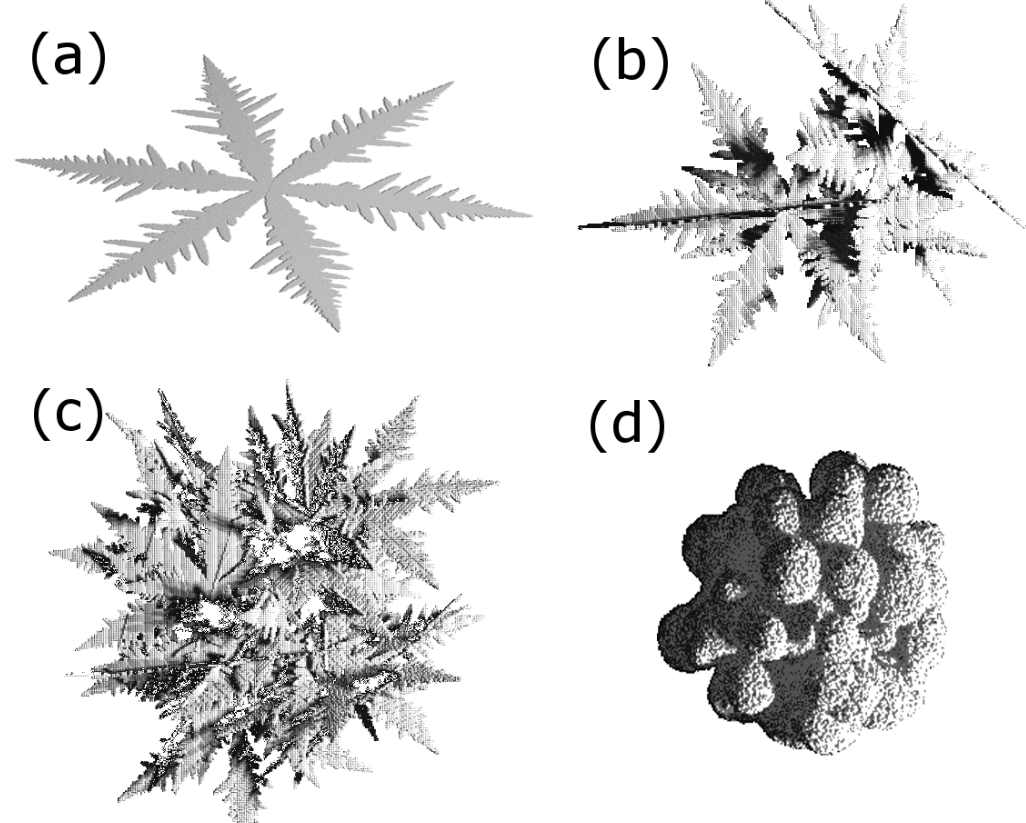


Figure 1. Selected shapes used in present study: (a) dendrite, (b) 5-flake aggregate, (c) 20-flake aggregate, and (d) graupel-like particle. Panels (b) and (c) are randomly oriented and translated copies of (a).

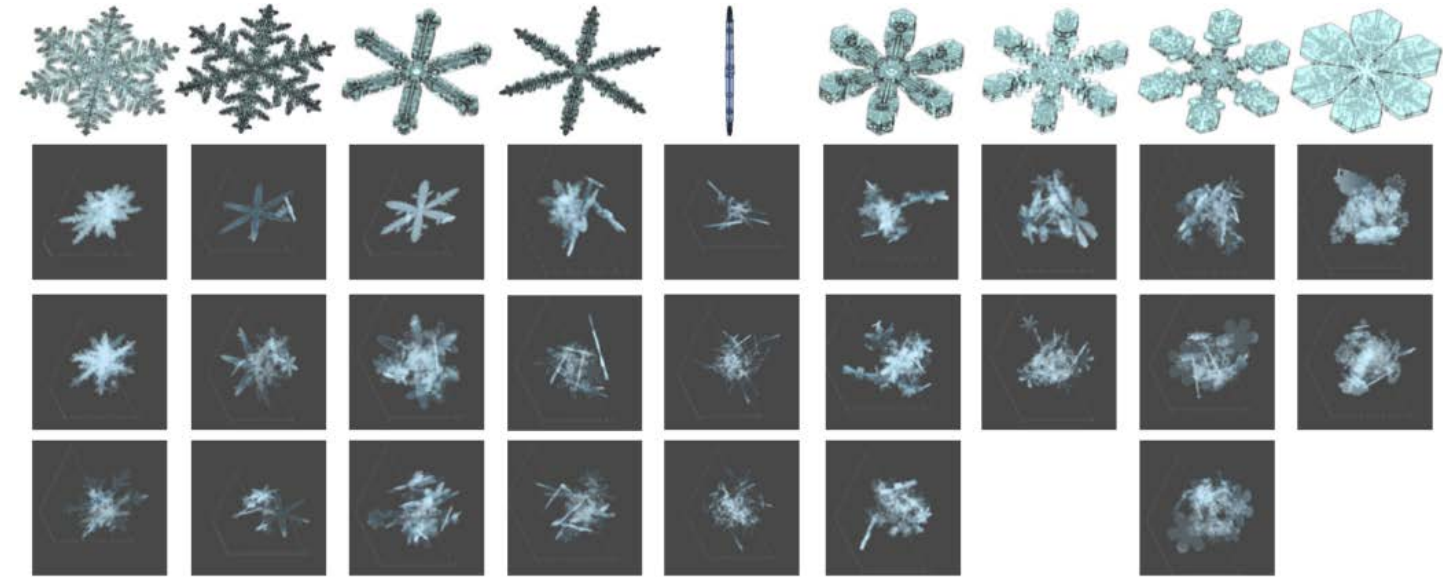


Figure 2. Simulated aggregates with their constituent base shapes (top row) and example aggregates consisting of various sizes of the base shape monomers (image from K.-S. Kuo).

2 Scattering and Extinction Properties

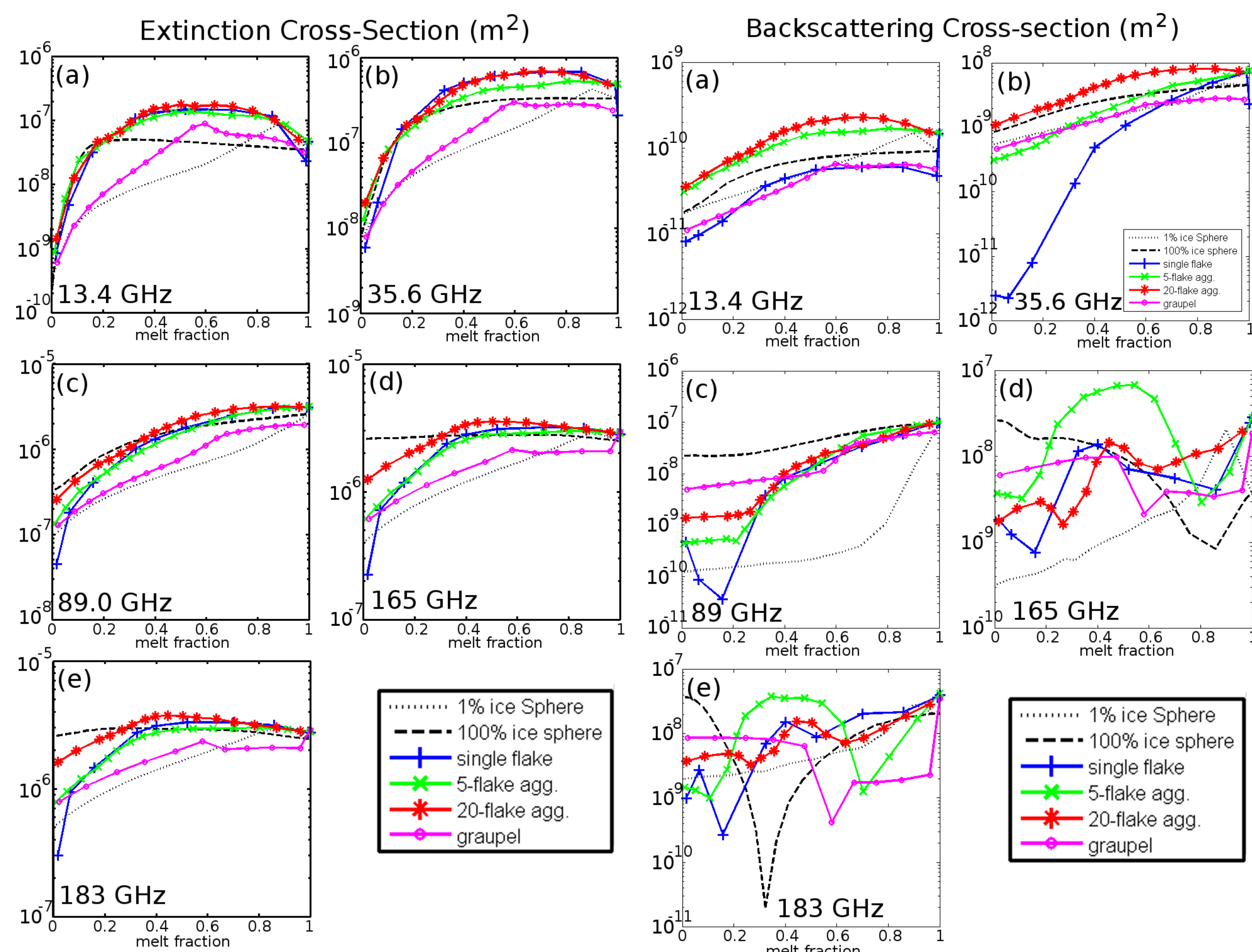


Figure 4. Extinction and backscattering cross-sections (m^2) versus melt fraction for the shapes from Fig. 1 at 13.4, 35.6, 89, 165, and 183.31 GHz. The mass of each particle is constant ($\sigma_{0i} = 500 \mu m$). Also shown for reference are curves for a 1% ice-air sphere, and a 100% ice (solid) sphere.

Acknowledgments:

This work is funded by the following NASA Grants: NNX11AR55G (PI: B. Johnson), NNX10AI49G (PI: W. Olson), and NNX10AT36A (PI: G. Skofronick-Jackson).

The code used to compute the scattering and absorption properties is an implementation of the discrete dipole approximation DDSCAT 7.2: Draine, B. T. & Flatau, P. J., 1994. "Discrete-dipole approximation for scattering calculations". J. Opt. Soc. Am., 11, 1491-1499.

The authors thank K.-S. Kuo for providing examples of simulated aggregates (Figure 2).

3 Simulations

Goal: Simulate observable quantities (in progress), such as reflectivity at radar frequencies, path integrated attenuation and passive microwave brightness temperatures.

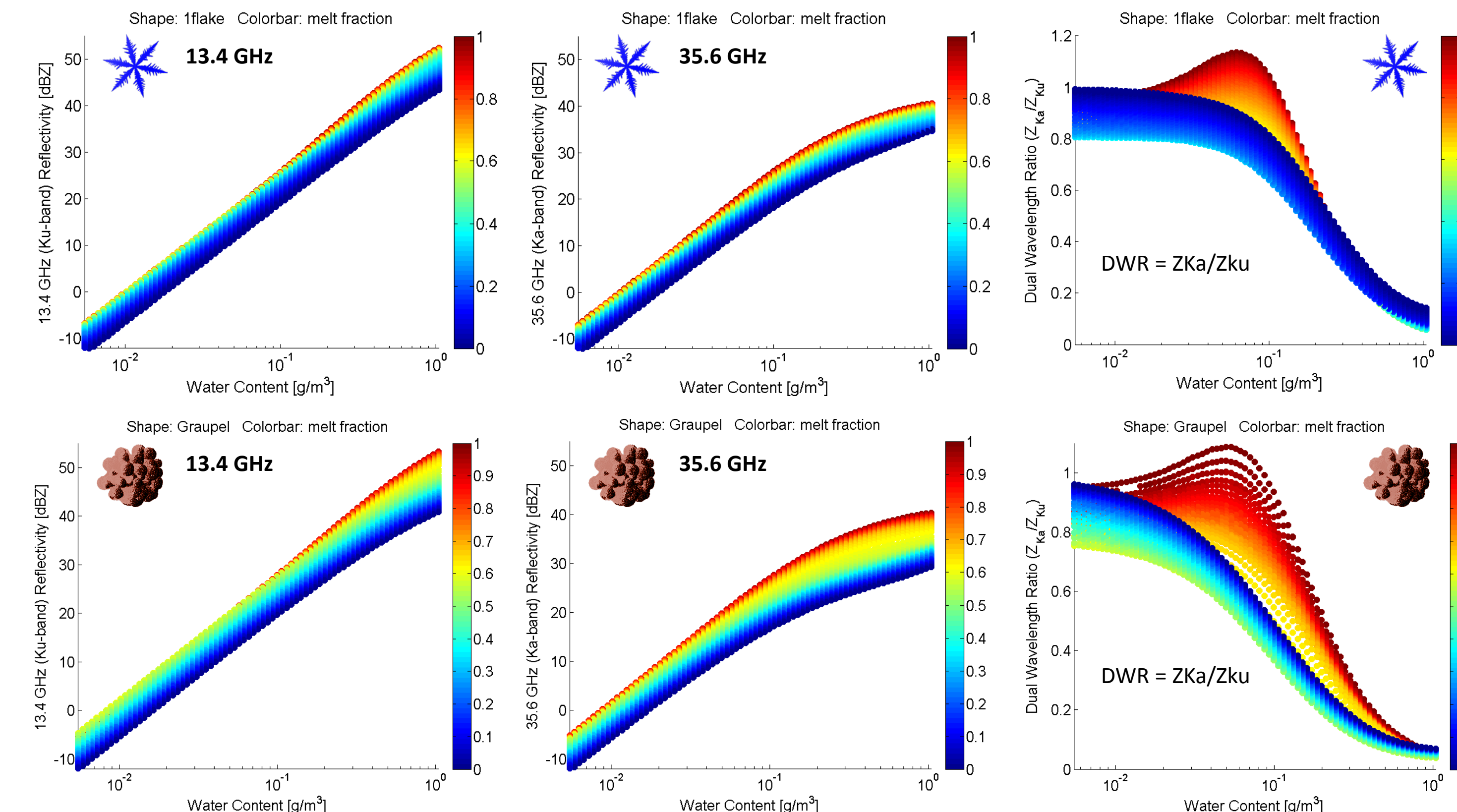


Figure 5. Radar reflectivity (unattenuated) vs. water content at Ku and Ka bands (13.4 and 35.6 GHz), the third column is the Dual Wavelength Ratio. Assumes exponential particle size distribution consistent with the findings of Sekhon-Srivastava (JAS, 1970). Row 1: single flake results, row 2: graupel results.

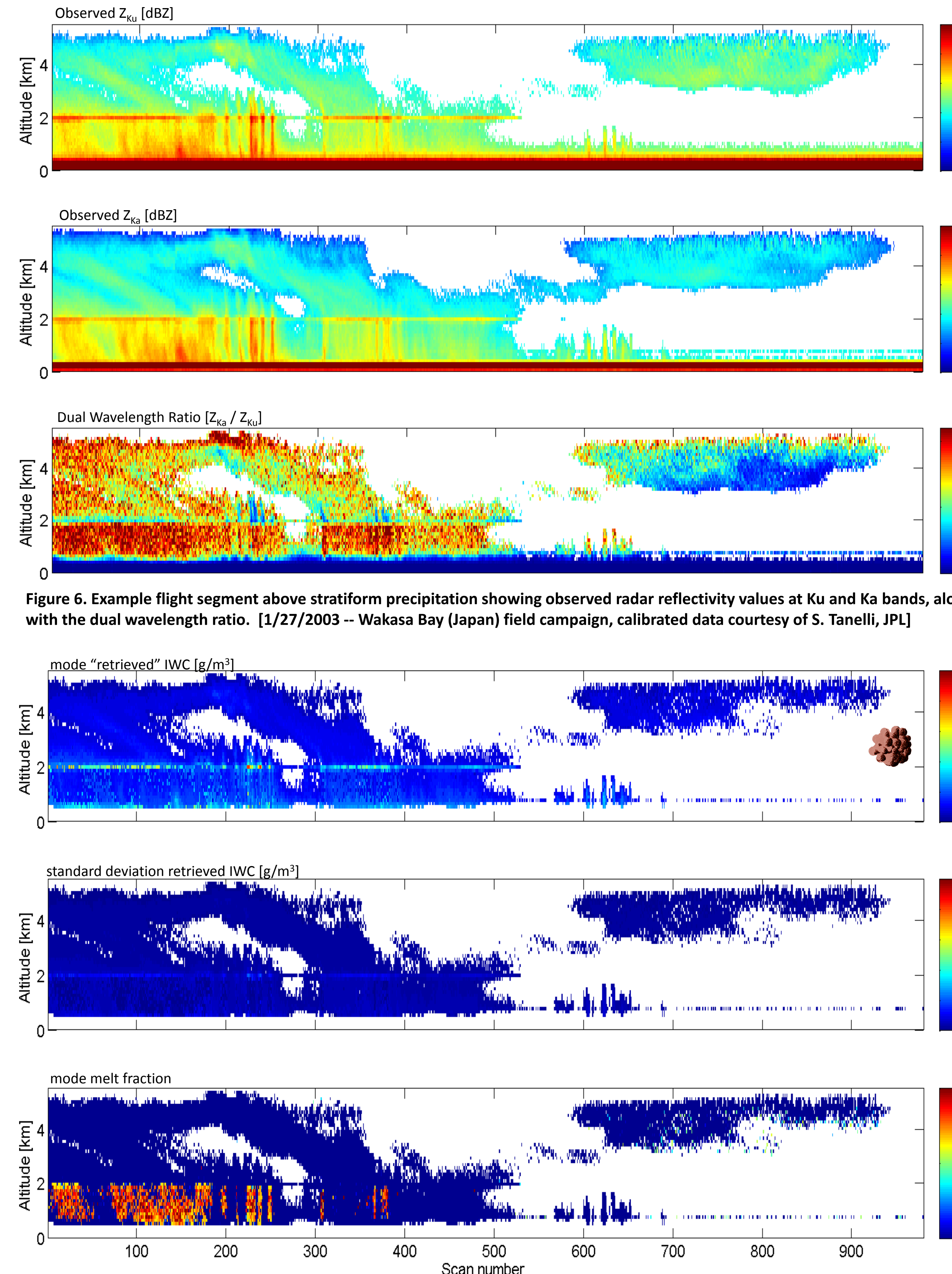


Figure 6. Example flight segment above stratiform precipitation showing observed radar reflectivity values at Ku and Ka bands, along with the dual wavelength ratio. [1/27/2003 - Wakasa Bay (Japan) field campaign, calibrated data courtesy of S. Tanelli, JPL]

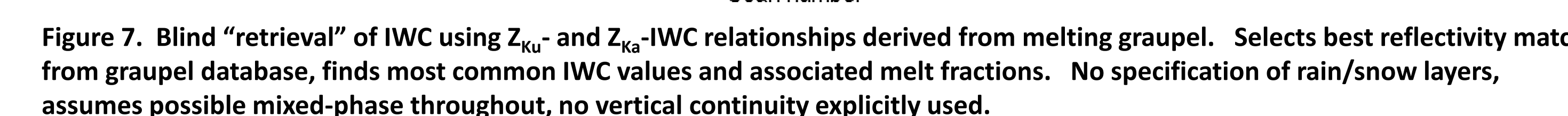


Figure 7. Blind "retrieval" of IWC using Z_{Ku} - and Z_{Ka} -IWC relationships derived from melting graupel. Selects best reflectivity match from graupel database, finds most common IWC values and associated melt fractions. No specification of rain/snow layers, assumes possible mixed-phase throughout, no vertical continuity explicitly used.

4 GPROF Channel Sensitivity Study

GPROF is the passive microwave radiometer algorithm for GPM, and will be used to retrieve precipitation rates based on comparisons with observed radar data. Snowfall is especially difficult to sense using passive microwave observations, so I performed a very simple sensitivity study to examine the effect of adding/removing particular channels from the retrieval. In this case study below, SSMIS observations of snowfall and a MMF-derived database are used for the retrieval. All examples are compared to the "baseline" (panel h).

The 11 SSMIS channels are: 19V, 19H, 22V, 37H, 37V, 91V, 91H, 150H, 183H±6, 183H±3, 183H±1

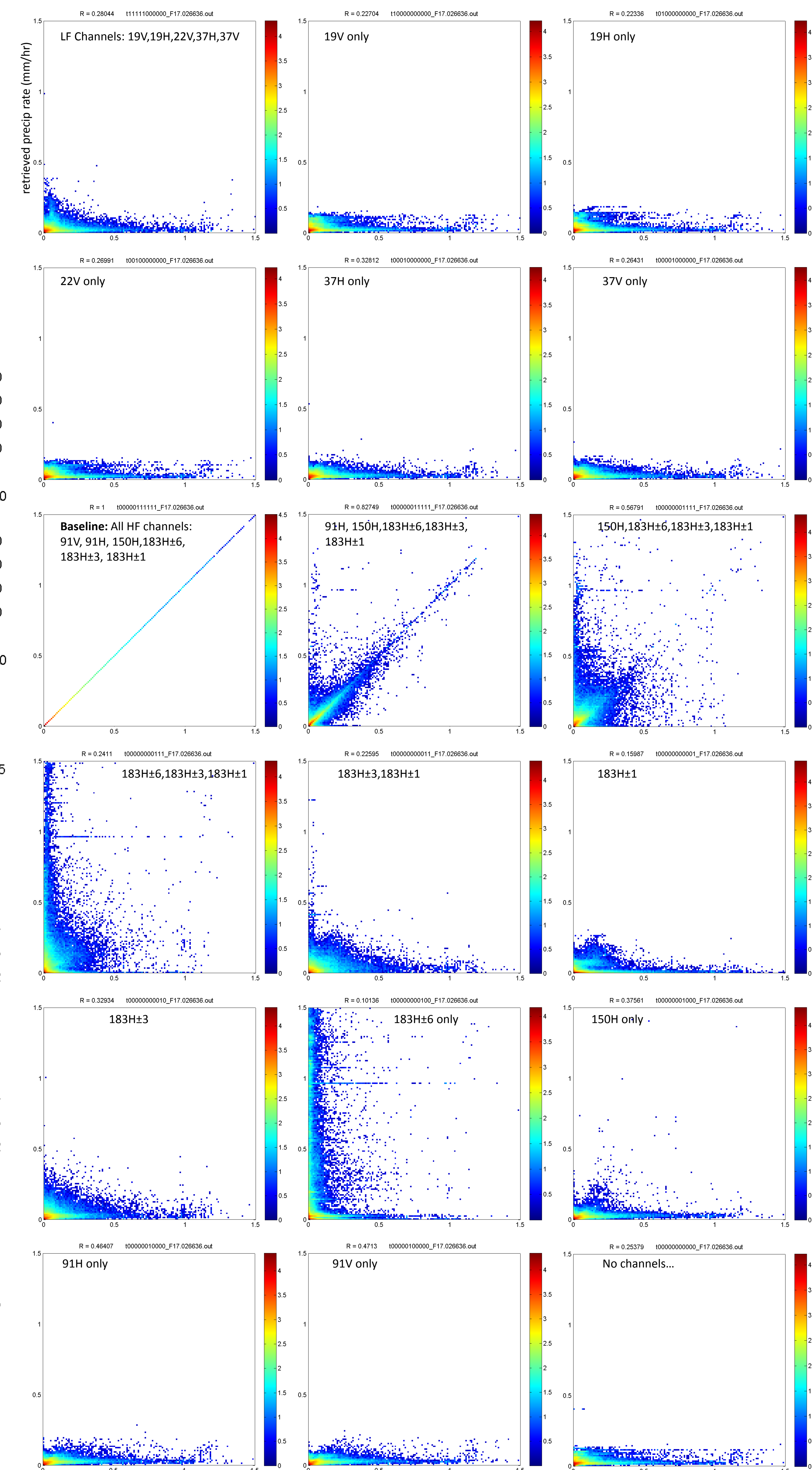


Figure 8. Sensitivity study plots showing retrieved precip rate (mm/hr) vs. water content for various channel combinations. The plots show the impact of removing or adding channels on the retrieval of precipitation rates.